Noise Removal in Lung LDCT Images by Novel Discrete Wavelet-Based Denoising With Adaptive Thresholding Technique

Shabana R. Ziyad, Prince Sattam bin Abdulaziz University, Saudi Arabia

Radha V., Avinashilingam Institute for Home Science and Higher Education for Women, India

Thavavel Vaiyapuri, Prince Sattam bin Abdulaziz University, Saudi Arabia

https://orcid.org/0000-0001-5494-5278

ABSTRACT

Cancer is presently one of the prominent causes of death in the world. Early cancer detection, which can improve the prognosis and survival of cancer patients, is challenging for radiologists. Low-dose computed tomography, a commonly used imaging test for screening lung cancer, has a risk of exposure of patients to ionizing radiations. Increased radiation exposure can cause lung cancer development. However, reduced radiation dose results in noisy LDCT images. Efficient preprocessing techniques with computer-aided diagnosis tools can remove noise from LDCT images. Such tools can increase the survival of lung cancer patients by an accurate delineation of the lung nodules. This study aims to develop a framework for preprocessing LDCT images. The authors propose a noise removal technique of discrete wavelet transforms with adaptive thresholding by computing the threshold with a genetic algorithm. The performance of the proposed technique is evaluated by comparing with mean, median, and Gaussian noise filters.

KEYWORDS

INTRODUCTION

Lung cancer is the second most common cancer in the USA [American Cancer Society. (n.d.)]. Some of the causes of lung cancer include smoking and inhalation of harmful chemical compounds generated by vehicles and industries. The detection of cancer at an early stage is a challenging task for radiologists. Some of the tests performed for diagnosing lung cancer include chest X-ray imaging, CT imaging, biopsy, and sputum cytology [Cancer Council Victoria. (n.d.)]. Chest X-ray is the primitive form of diagnosis of lung related diseases and the next generation witnessed the development of more effective diagnosing test, the X-ray CT. The X-ray CT technique, however, had drawbacks of exposure to high doses of radiation. This health hazard was one of the serious predicaments that demanded urgent attention from researchers. The scientific advancement in the field of imaging tests led to the introduction of Low Dose Computed Tomography (LDCT) as a preferred imaging modality for patients with lung diseases. This development proved to be a breakthrough in the diagnosis of lung cancer.

Among the existing CT imaging techniques, LDCT imaging provides good-quality images while exposing the patient to a low dose of radiation. In the National Lung Screening Trial (NLST), the

radiation dose given to patients in LDCT screening test is 2 mSv, compared to the radiation dose for full-chest CT scan which is approximately 8 mSv in the diagnostic study intended to follow up the detection of nodules in patients with lung cancer (McCunney & Li, 2014). The NLST study revealed that annual screening of heavy smokers with LDCT reduced the death rate from lung cancer by 20% compared to screening by conventional chest X-ray (Schabath et al., 2016). LDCT technique has a shortcoming of generating noisy image. The noise is induced in the image due to various factors such as reduced radiation dose, machine calibration, and reconstruction algorithms.

Multimedia techniques in Health care allows the patient related data such as images, texts, audio and video to be stored and processed efficiently (Rathee et al., 2020). LDCT images are stored in Digital Imaging and Communications in Medicine (DICOM) format. This is an international standard developed for storage and transmission of the medical images. LDCT images are a challenge to radiologists in detecting nodules that are minute and camouflage with the vessels and the background region. An automated Computer-Aided Diagnosis (CADx) proves to be one of the efficient tools to aid radiologists in detecting lung nodules accurately. CADx includes five phases: preprocessing, segmentation of the region of interest, feature analysis, classification, and performance analysis.

The preprocessing step involves improving the quality of the images under study, which in turn improves the subsequent phases of the CADx. In this study, preprocessing is carried out to eliminate noise in LDCT images and enhance the contrast of these images to boost the performance of the CADx. The section "Noises in LDCT Images" describes the noise prevalent in LDCT images. The "Related Work" section throws light on literature related to this topic. The section "Theoretical Background" discusses the types of existing denoising filters, the mathematical concept of wavelets, Discrete Wavelet Transform (DWT), and denoising method using DWT. The subsequent section discusses the proposed algorithm for denoising LDCT images. The section on experimental results tabulates the results of preprocessing.

NOISES IN LDCT IMAGES

The artifacts in the LDCT images can be classified as patient-related artifacts [Hacking & Cuete (n.d.)], machine-related artifacts, and transmission-related artifacts (Boas & Fleischmann, 2012). Patient-related artifacts include slight movement of the patients undergoing the tests and the body temperature of the patient. Machine-related artifacts include device calibration error, reducing the X-ray flux, and partial volume effects. Transmission-related artifacts occur during the transmission through the communication channel. Noise prevalent in LDCT images is found to be Quantum noise or Poisson noise (Manson et al, 2019) and Gaussian noise (Goyal et al., 2018). Quantum noise originates in LDCT images depending upon the photon count that impinges on the surface of the image receptor from the X-ray source. Photons impinging on the image receptor cannot be equally distributed by any technique, as it is a random process. This random distribution generates Quantum noise. The name arises from the fact that a photon is a quantum of energy. The photon count that falls on the detector is inversely proportional to the noise generated in the image. When the photon count reaches zero, the regions of the image are found to be afflicted with Quantum noise.

The radiation dose has a considerable impact on the level of Quantum noise. A trade-off should be maintained between the radiation dose and the image noise. The radiation dose, to which patients with lung cancer are exposed, is inversely proportional to the noise in the image. Therefore increasing the radiation dose reduces the noise in the images. Reducing the radiation dose by a factor of n increases the noise in image by $\sqrt{n}$. The Quantum noise and the electronic Gaussian noise in the images should be reduced considerably alongside preserving the edges of the image.

RELATED WORK

The preprocessing phase of CADx for lung nodule classification as benign or malignant includes the phases: noise removal and contrast enhancement. Noise removal in LDCT images was performed by several techniques grouped into four categories: filter-based methods, transformation-based techniques, model-based techniques, and deep learning-based techniques. In the filter-based technique, a Gaussian filter is adopted for the smoothing of LDCT images with Gaussian noise in the preprocessing step (Camarlinghi, 2013). Image preprocessing techniques of the median filter and the Histogram Equalization (HE) eliminate primary noise and image distortion (Farahani et al., 2015). Non-Local Means (NLM) algorithm for denoising Poisson noise was adopted by eminent researchers (Green et al. 2017; Wang et al., 2017; Zhang et al., 2017). A new transformation-based technique in Tetrolet transform was adopted for denoising Gaussian noise (Kumar & Diwakar, 2016). A denoising method based on DWT, and a modified median filter was proposed (Chen et al., 2019). A modified Rudin–Osher–Fatemi (ROF) model is found to be effective in denoising images corrupted by additive white Gaussian noise (Amer et al., 2019). A convolutional neural network auto encoder-decoder is employed for LDCT image noise reduction. This method integrates the CNN, Autoencoder, and Residual learning and Parametric Rectified Linear Unit (Mao & Zhao, 2020). Figure 1 shows the classification of the denoising techniques for LDCT images. The preprocessing and segmentation of the MRI images are carried out using hybrid k-means graph cut technique (Dogra et al., 2018).

Figure 1. Classification of the denoising techniques for Lung LDCT images
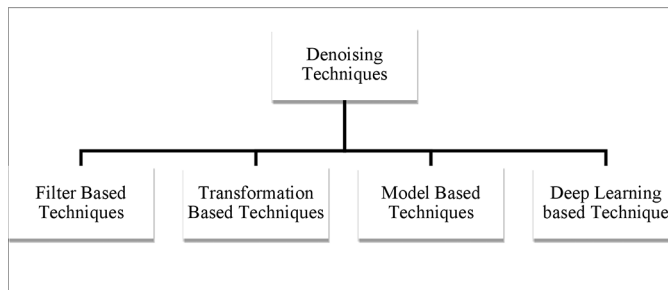
THEORETICAL BACKGROUND

Filters Adopted for Denoising in Medical Images

The various filters used for noise removal include the Mean, Median, Gaussian, NLM, and Bilateral filters which has the ability to efface the noise in images. The disadvantage lies in the blurring of edges that occurs due to the smoothing operation of the filters. Edge detection is an important operation in image processing and pattern recognition. Edges capture the vital features of any image (Sharma et al., 2017). Therefore, there is pressing need to develop a denoising technique which preserves the edges from smoothing.

Mean Filter

A mean filter, also known as an average filter, is one of the popular filters used for denoising images. In the Mean filter, the kernel is a square window of size n that slides on the LDCT image replacing the pixels. Every pixel value of varying intensity compared to the eight neighborhood pixel values will be replaced by the average of the surrounding pixel values.

Median Filter

The median filter is a nonlinear filtering technique used frequently in the field of medical imaging. In the Median filter, the pixel intensity of the image that is an outlier which is replaced with a median value of the neighborhood regions. Outliers are identified by examining the intensity of the neighborhood pixels. Median filters possess the property of preserving edges as compared to Mean filters. In this technique the histogram intensity is computed for each neighborhood, following which the median is computed and the pixel is updated. Sorting of the neighboring pixels is performed by Bubble sort. Some improved versions of this filter are the weighted median filter, tri-state median filters, and decision-based median filters (Shrestha, 2014).

Gaussian Filter

Gaussian filter is a low-pass filter used for image denoising in the field of image processing. Although the filter possesses the features of noise reduction, it blurs the edges and details as it smoothes the image. It is mainly applied to remove noise in the image where the noise shows a normal distribution as given in Equation 1:

$$G\left(x, y, \mu, \sigma\right) = \frac{1}{2\pi\sigma^2} \exp\left[\frac{-\left(x - \mu_1\right)^2 - \left(y - \mu_2\right)^2}{2\sigma^2}\right] \tag{1}$$

where σ is the distribution width or SD and μ_1 and μ_2 are the mean values of the distribution. The Gaussian filter possesses a weight distributed in a manner that gives a higher significance to the edges. The smoothing effect of the filter relies on the parameter σ. The Gaussian filter works well when the noise in the image shows a Gaussian distribution (Seddik, 2014). The Gaussian kernel coefficients are designed on the basis of the Gaussian function as shown in Equation 2:

$$G\left(x, y\right) = \frac{1}{2\pi\sigma} e^{\frac{x^2 + y^2}{2\sigma^2}} \tag{2}$$

in which the distribution has a mean value of zero. The continuous Gaussian function is mapped to a kernel with discrete values. The kernel of the Gaussian filter is designed to have higher weights at the center and weights diminishing while radiating toward the edges of the kernel.

Every pixel in the image was replaced by the average pixel intensity of the image multiplied by the weighted kernel placed over the image. It results in blurring the edge details in the image by replacing aberrant edge pixels with the intensity of the neighboring pixels. This filter can remove Gaussian noise found in medical images, but due to its drawback of blurring edges, not used in any CADx as a denoising technique.

Genetic Algorithm

One of the biologically inspired algorithms is the Genetic Algorithm (GA) that was developed on the basis of Charles Darwin's theory of evolution. GA takes the essence of the natural evolution of the species through mating and survival of the fittest. GA is a heuristic search methodology that finds application in large areas involving optimization problems. The GA involves the following phases: the selection of a population of chromosomes, evaluation of their fitness with fitness function, ranking the parents, selection of the best parents for crossover, and mutation to generate a new population for the next iteration. The algorithm begins with the selection of possible solutions or candidates called population for the optimization problem under study. These potential candidates are assessed for fitness

by a ranking method. The evaluation of the ranking method is performed by the fitness function that is unique for every optimization problem. The selection step selects the best potential candidates as part of the population. Crossover is the process where the genes of two or more parents are combined to evolve a new candidate with a higher fitness ranking. The objective of the crossover stage is to generate a population that is closer to the optimum solution compared to the existing candidates in the population. Mutation creates random changes in the candidate solutions after crossover. The mutation operator should possess the features of reachability, unbiasedness, and scalability. The termination criterion is usually the convergence of the optimum solution, whereas in some cases, it also executes for a predefined number of iterations to minimize the computational costs (Kramer, 2017).

Wavelets

A wave is an oscillating function of time or space as a sinusoid. A wavelet is a small finite wave that has energy for a stipulated amount of time and acts as a tool to analyze any non-stationary signals varying with time. It allows analysis in both time and frequency domains. Wavelets are a boon to researchers working in the field of medical imaging. Applications of wavelets are the areas of image denoising, image compression, and feature extraction from medical images.

Wavelet has broad clinical applications in the field of medical images as they can identify any abrupt changes in an image, specifically in the edge regions of the image, by two basic operations of scaling and shifting. The scaling of the wavelet results in shrinking and expanding the frequency of the wavelet. When the scaling factor of the wavelet decreases, the frequency of the wavelet increases, and it captures all the minute changes in the images. When the scaling factor increases, the frequency of the wavelet decreases, and abrupt or sudden changes in the image captured by the wavelet.

Discrete Wavelet Transform

Discrete Wavelet Transform (DWT) is a discretized wavelet and is an advanced concept compared to the traditional Fourier transform. DWT is a computational method for denoising electrical signals. The representation of signal $f(t)$ is given in Equation 3.

A signal is represented as:

$$f\left(t\right) = \sum_{l} a_l \psi_l \left(t\right) \tag{3}$$

where l is an integer index, a_l is the real valued expansion coefficient, and $\psi_l\left(t\right)$ is set of function of t.

The same function with respect to two dimensions for images may be represented as $f\left(t\right)$ shown in Equation 4:

$$f\left(t\right) = \sum_{k}\sum_{j} a_{j,k} \psi_{j,k}\left(t\right) \tag{4}$$

where j and k are integers and $\psi_{j,k}\left(t\right)$ is a wavelet expansion function.

Let φ and ψ^{2D} represent the scaling function and 2D wavelet.

The scaling function in 2D is then represented as φ^{2D} and given in Equation 5:

$$\varphi^{2D}\left(x,y\right) = \varphi\left(x\right)\varphi\left(y\right) \tag{5}$$

and three wavelets are given in Equations 6, 7, and 8:

$$\psi_1^{2D}\left(x,y\right) = \varphi\left(x\right)\psi\left(y\right) \tag{6}$$

$$\psi_2^{2D}\left(x,y\right) = \psi\left(x\right)\varphi\left(y\right) \tag{7}$$

$$\psi_3^{2D}\left(x,y\right) = \psi\left(x\right)\psi\left(y\right) \tag{8}$$

In 2D wavelet decomposition, the two objects obtained are the approximation and detail coefficients of spaces. For an image X, a signal in 2D, the image is decomposed into a different resolution scale as given in Equation 9:

$$X = A_j + D_j + A_{j-1} + D_{j-1} + \dots A_1 + D_1 \tag{9}$$

The detailed band decomposed in three directions, namely horizontal, vertical, and diagonal, as shown in Equations 10 and 11:

$$A_{j-1} = A_j + D_j \tag{10}$$

$$A_{j-1} = A_j + D_j = A_j + \left[\left(D_h\right)_j + \left(D_v\right)_j + \left(D_d\right)_j\right] \tag{11}$$

where $D_h, D_v,$ and D_d indicate the horizontal, vertical, and diagonal details, respectively. The image undergoes the first level of decomposition along the rows and columns to generate the approximation coefficient A and detail coefficients H, V, and D, which are the horizontal, vertical, and diagonal coefficients, respectively. If the image size is 256×256, it will result in four images of size 128×128. In the second level of decomposition, the approximation coefficient A has been decomposed by DWT to yield the approximation and the detailed coefficients (Misiti et al., 2007). Level-wise decomposition of the images after applying DWT is shown in Figure 2.

Denoising With Discrete Wavelet Transform

Practical applications of DWT include some imaging processing tasks such as fusion, compression, edge detection, and denoising of images. Image denoising is one of the well-known applications of the DWT and is discussed in this section. The Dicom image with noise is $X\left(i,j\right)$. The Dicom image to be retrieved after denoising is $Y\left(i,j\right)$. In general, $X(i,j)$ can be written as shown in Equation 12:

$$X\left(i,j\right) = Y\left(i,j\right) + \in_{i,j} \tag{12}$$

Figure 2. Three levels discrete wavelet decomposition of Dicom images
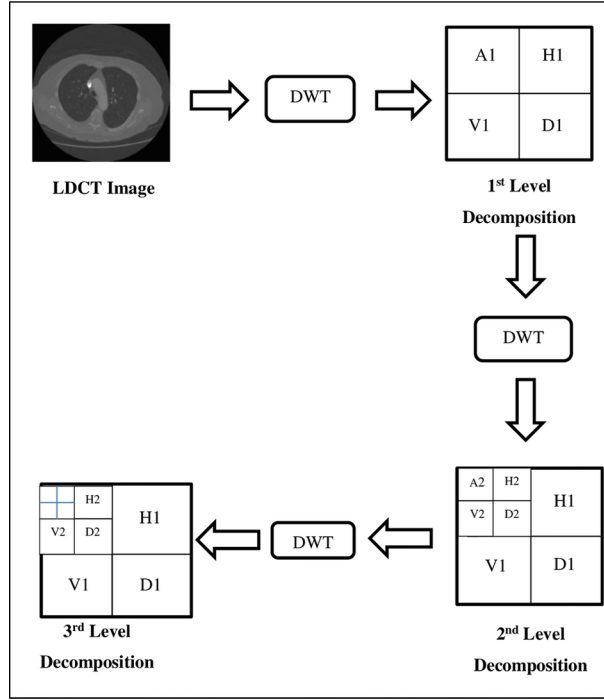
where $\in$ is Quantum noise or Gaussian noise with covariance matrix $\sigma^2 I$. The denoising of the Dicom images is performed with the following three steps. DWT is applied on the rows and columns of the image where low-pass and high-pass filters are applied on the images to retrieve four coefficients. The low-pass filter generates the approximation coefficient as the output, and the high-pass filters generate the detailed images that represent the horizontal, vertical, and diagonal coefficients of the image. This process can be repeated to multilevel according to the level of noisy images in various applications.

Step 1: Applying DWT on the image at the nth level of decomposition.
Step 2: Thresholding the detail coefficients H, V, and D with the optimal threshold value dependent on σ. The thresholding value is estimated using the universal thresholding method. In universal thresholding, T is calculated as shown in Equation 13:

$$T = \sigma\sqrt{2\log N \times N} \tag{13}$$

where N is the image size and σ is given in Equation 14:

$$\sigma = \frac{\text{Median}\left|w_n^j\right|}{0.6745} \forall j \text{ diagonal coefficients} \tag{14}$$

where w_n^j is the wavelet coefficient in scale n.

Step 3: Reconstructing the denoised Dicom image with the approximation coefficients and detailed coefficients from the nth level.

PROPOSED ALGORITHM FOR DENOISING LDCT IMAGES

The DWT algorithm for noise reduction varies in the method of calculating the threshold value according to the applications. Thresholding selection in denoising is performed by soft thresholding or hard thresholding. In both these thresholding techniques, the noise above a certain threshold is clipped and reduced below the threshold levels; the difference lies in the approach by which the noisy pixels having noise level below the threshold are treated. They are reduced to an optimum level in soft thresholding but retained in their original form in hard thresholding. Some researchers have proposed adaptive thresholding methods for denoising (Borsdorf et al., 2008) and combining filters such as Median filter with DWT for denoising (Chen et al., 2019).

Threshold Level Estimation

The threshold level estimation for images is performed by GA (Goldberg, 1989). GA randomly initializes the set of possible solutions for the problem under consideration as the population. The solutions in the population are known as chromosomes that are composed of genes. Every GA requires a fitness function to evaluate the probability of the chromosome. After the evaluation of the fitness of the chromosomes, they are ranked according to their fitness. The best fit chromosomes form the part of the next generation of the population. The crossover and mutation operation is performed to avoid the GA to converge to the optimum solution in a few iterations and to increase the search space to find the optimum solution.

In this study, the process of finding the optimal threshold value for the soft thresholding process of the approximation and detailed subbands of the image is performed with the GA. The fitness function for the GA is customized according to the study. The Mean Square Error (MSE) of the original image and denoised image in each of the iteration is the fitness function to be optimized in selecting the threshold for proposed denoising algorithm. The fitness function used for finding the best chromosome in the population is the MSE calculated as shown in Equation 15:

$$\mathrm{MSE}\left(X, Z\right) = \sum_{i=1}^{m}\sum_{j=1}^{n}{X_{i,j}} - {Z_{i,j}}^2 \tag{15}$$

where $X_{i,j}$ is the restored image and $Z_{i,j}$ is the original image of size $m \times n$. The methodology for threshold estimation is shown in Figure 3. Following the implementation of this procedure, the optimal value is reached after 15 to 20 iterations in each level of decomposition. In the algorithm GA parameters are set as 0.1 for the selection probability, 0.8 for crossover probability and 0.1 for mutation probability. The optimum threshold value calculated is the parameter to perform the soft thresholding operation. This method of thresholding proves to be more efficient in denoising the images than the universal threshold method.

Algorithm for Denoising in LDCT Lung Images

The preprocessing stage of the CADx has a precise objective of improving the quality of images and enhancing the images by reducing their degradation due to Quantum and Gaussian noise. To achieve this objective, a novel method of multilevel decomposition of LDCT images by applying

Figure 3. Flowchart for threshold computation
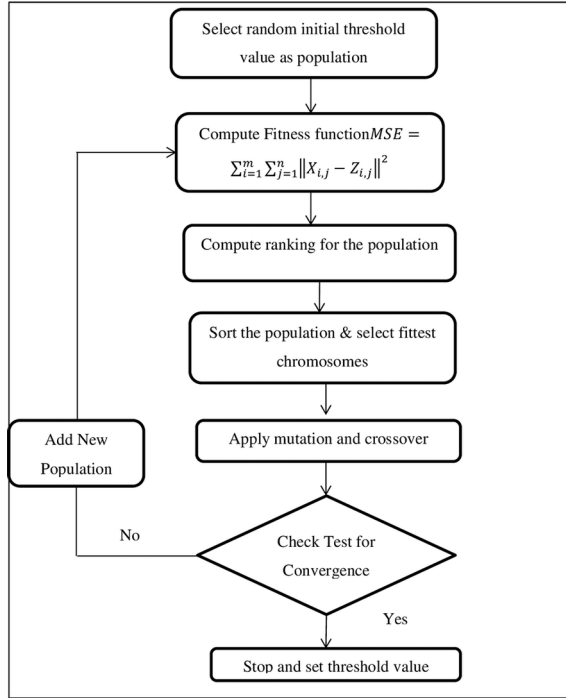
DWT, followed by thresholding the image with adaptive soft thresholding and reconstructing the image by applying inverse of DWT starting from the third level has been proposed in this section. The threshold level is usually selected by the novel methodology for estimating the threshold based on the GA. The threshold level is set to the optimal value in each of the decomposition levels. The proposed algorithm for the denoising of LDCT images – Discrete Wavelet Transform with Adaptive Thresholding (DWTWAT) – is described in this section.

Step 1: Apply DWT on the image at the first level of decomposition by using Daubechies wavelet. Retrieve four images: one approximate image and three detailed images $I_1^{1D}, I_2^{1D}, I_3^{1D}$, and I_4^{1D}.

Step 2: Apply DWT on the approximation image I_1^{1D}. Retrieve four images: one approximate image and three detailed images $I_1^{2D}, I_2^{2D}, I_3^{2D}$, and I_4^{2D}.

Step 3: Apply again DWT on the approximation image I_1^{2D}. Retrieve four images: one approximate image and three detailed images $I_1^{3D}, I_2^{3D}, I_3^{3D}$, and I_4^{3D}.

Step 4: For each level j of decomposition.

Step 4.1: The optimum threshold value T_1^{jD} is computed using the GA-based technique.

Step 4.2: The detailed images I_2^{jD}, I_3^{jD}, and I_4^{jD} undergo the soft thresholding process with the optimum threshold value T_1^{jD} calculated.

Step 5: Inverse of DWT is applied on the processed images $I_1^{jD}, I_2^{jD}, I_3^{jD}$, and I_4^{jD} at each jth level of decomposition by using Daubechies wavelet starting from the jth level.

EXPERIMENTAL RESULTS

A dataset of 25 sample LDCT lung images was acquired from the Lung Image Database Consortium-Image Database Resource Initiative (LIDC-IDRI) public database ([Cancer Imaging Archive. (n.d.)].). The performance evaluation of the denoising techniques in MRI images was performed with parameters MSE and Peak Signal Noise Ratio (PSNR) (Tiruwa & Yadav, 2018). The quantitative evaluation of the wavelet based two stage denoising method for ultrasound medical images was carried out using the metrics of MSE, PSNR, and SSIM (Periyasamy & Ramasamy, 2018).In this research study the commonly used Mean, Median, and Gaussian filters are compared with the proposed methodology by using the parameters of MSE and PSNR. MSE and PSNR are given as Equations 16 and 18. The MSE is the measure of the cumulative squared error between the denoised LDCT image $Y(i,j)$ and the original LDCT image $X(i,j)$ with size $M{\times}N$:

$$\text{MSE} = \sum \left(Y\left(i, j \right) - X\left(i, j \right) \right)^2 M{\times}N \tag{16}$$

PSNR is defined as the ratio between the maximum possible power of a signal and the power of corrupting noise. It is measured in decibels (dB). The formula for Root Mean Square Error (RMSE) and PSNR are given in Equations 17 and 18:

$$\text{RMSE} = \sqrt{\text{MSE}} \tag{17}$$

$$\text{PSNR} = 20\log_{10} 255^2 \, \text{RMSE} \tag{18}$$

Table 1 shows the results of MSE and PSNR on applying the Mean, Median, Gaussian filters, and the proposed algorithm DWTWAT on the sample dataset. Table 2 shows the LDCT images after applying the four filters. Figure 4 shows the graph for the performance evaluation of DWTWAT according to MSE. Figure 5 shows the graph for the performance evaluation of DWTWAT according to PSNR measured in dB.

DISCUSSION OF RESULTS

The existing techniques of Mean, Median and Gaussian filters are applied on the sample dataset of 25 LDCT lung images. The experimental result shows that the average MSE value for selected dataset

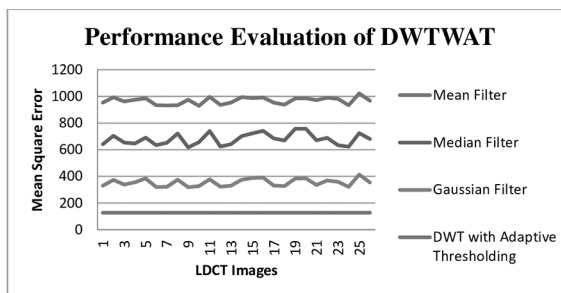**Figure 4. Performance evaluation of DWTWAT with the existing techniques according to MSE**

Figure 5. Performance evaluation of DWTWAT with the existing techniques according to PSNR
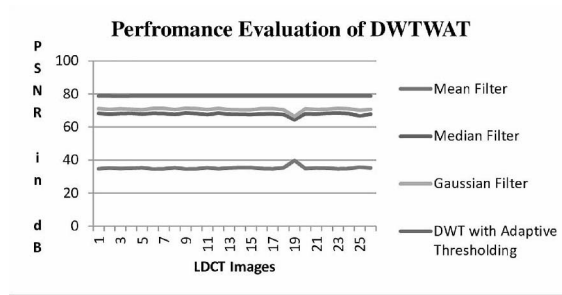

Table 1. Comparison of DWTWAT with existing filters according to MSE and PSNR (in dB)

Image No.	MSE				PSNR			
	Mean Filter	Median Filter	Gaussian Filter	DWTWAT	Mean Filter	Median Filter	Gaussian Filter	DWTWAT
1	953.35	641.64	330.51	126.94	34.78	68.25	71.13	78.81
2	993.64	704.79	373.06	126.96	35.22	67.84	70.61	78.83
3	961.59	654.27	338.53	126.96	34.89	68.17	71.03	78.70
4	974.22	646.87	356.00	126.95	35.05	68.22	70.81	78.82
5	986.12	690.44	384.94	126.96	35.36	67.93	70.47	78.83
6	934.57	633.84	320.19	126.97	34.67	68.30	71.27	78.84
7.	932.68	652.02	321.47	126.95	34.69	68.18	71.25	78.82
8	934.01	721.78	375.42	126.95	35.25	67.74	70.58	78.82
9	974.60	617.30	318.54	126.96	34.64	68.42	71.29	78.83
10	929.19	656.11	327.26	126.96	34.76	68.15	71.18	78.83
11	995.87	739.66	377.71	126.94	35.25	67.63	70.55	78.81
12	936.84	624.70	323.38	126.97	34.71	68.37	71.23	78.84
13	953.35	641.64	330.51	126.94	35.24	67.86	70.58	78.81
14	994.74	701.95	375.26	126.94	35.38	67.73	70.43	78.82
15	987.28	723.68	388.59	126.95	35.42	67.63	70.41	78.83
16	992.34	741.07	390.14	126.96	34.79	67.97	71.13	78.83
17	953.08	684.27	330.77	126.96	34.75	68.07	71.18	78.82
18	937.80	669.77	327.15	126.95	35.28	67.53	70.49	78.83
19	985.40	757.12	383.08	126.96	39.71	64.36	66.38	78.84
20	986.54	756.42	384.89	126.97	34.84	68.06	71.06	78.82
21	972.15	670.42	336.09	126.95	35.20	67.94	70.65	78.83
22	989.84	689.63	369.63	126.96	35.10	68.30	70.76	78.82
23	982.56	634.52	360.01	126.95	34.70	68.38	71.25	78.83
24	934.42	623.34	321.68	126.96	34.87	68.15	71.03	78.81
25	1022.92	724.41	413.78	126.95	35.61	66.69	70.16	78.81
Average	**967.96**	**680.06**	**354.34**	**126.95**	**35.20**	**67.83**	**70.67**	**78.81**

Table 2. Experimental results of denoising by the tested filters

Original Image	Mean Filter Image	Median Filter Image	Gaussian Filter Image	DWTWAT Image

for the existing methods of the Mean, Median and Gaussian filters are 967.96, 680.06 and 354.34 respectively. The average PSNR value for the existing techniques of the Mean, Median and Gaussian filters are 35.20 dB, 67.83 dB and 70.67 dB. Comparison of the existing techniques of denoising revealed that the proposed method of DWTWAT has a low MSE value of 126.95 and a high PSNR value of 78.81 dB compared to the existing techniques under study. Images with low MSE and high PSNR value are considered as better quality images.

CONCLUSION

Medical imaging is one of the current research areas that demands efficient methods and techniques in the areas of image denoising, image compression, and feature extraction. There is a need to develop efficient denoising algorithms to improve the performance of automated disease detection tools and to reduce the radiological errors induced by low-quality images. Several researchers have proposed novel algorithms with the wavelet transform, including curvelet and shearlet. The proposed techniques of DWTWAT technique were shown to provide denoised LDCT images that could be used by doctors and radiologists for diagnosing lung cancer. As a future direction of research work, application of curvelets is proposed, this can preserve the curved structures in the images, for denoising of LDCT images.

ACKNOWLEDGMENT

REFERENCES

Amer, H. M., Abou-Chadi, F. E. Z., Kishk, S. S., & Obayya, M. I. (2019). A CAD system for the early detection of lung nodules using computed tomography scan images. *International Journal of Online and Biomedical Engineering*, *15*(4), 40–52. doi:10.3991/ijoe.v15i04.9837

American Cancer Society. (n.d.). *Key Statistics for Lung Cancer.* https://www.cancer.org/cancer/lung-cancer/about/key-statistics

Boas, F. E., & Fleischmann, D. (2012). CT artifacts: Causes and reduction techniques. *Imaging in Medicine*, *4*(2), 229–240. doi:10.2217/iim.12.13

Borsdorf, A., Raupach, R., Flohr, T., & Hornegger, J. (2008). Wavelet based noise reduction in CT-images using correlation analysis. *IEEE Transactions on Medical Imaging*, *27*(12), 1685–1703. doi:10.1109/TMI.2008.923983 PMID:19033085

Camarlinghi, N. (2013). Automatic detection of lung nodules in computed tomography images: Training and validation of algorithms using public research database. *The European Physical Journal Plus*, *128*(9), 110–114. doi:10.1140/epjp/i2013-13110-5

Cancer Council Victoria. (n.d.). *Lung cancer.* https://www.cancervic.org.au/cancer-information/types-of-cancer/lung_cancer/diagnosing_lung_cancer.html

Cancer Imaging Archive. (n.d.). *LIDC-IDRI.* https://wiki.cancerimagingarchive.net/display/Public/LIDC-IDRI

Chen, B., Cui, J., Xu, Q., Shu, T., & Liu, H. (2019). Coupling denoising algorithm based on discrete wavelet transform and modified median filter for medical image. *Journal of Central South University*, *26*(1), 120–131. doi:10.1007/s11771-019-3987-9

Dogra, J., Jain, S., & Sood, M. (2018). Segmentation of MR images using hybrid k mean-graph cut technique. *Procedia Computer Science*, *132*, 775–784. doi:10.1016/j.procs.2018.05.089

Farahani, F. V., Ahmadi, A., & Zarandi, M. H. F. (2015). Lung nodule diagnosis from CT images based on ensemble learning. In *IEEE Conference on Computational Intelligence in Bioinformatics and Computational Biology (CIBCB)* (pp. 47–53). doi:10.1109/CIBCB.2015.7300281

Goldberg, D. (1989). *Genetic Algorithms in Search, Optimization, and Machine Learning*. Addison-Wesley Longman.

Goyal, B., Dogra, A., Agrawal, S., & Sohi, B. S. (2018). Noise issues prevailing in various types of medical images. *Biomedical & Pharmacology Journal*, *11*(3), 1227–1237. doi:10.13005/bpj/1484

Green, M., Marom, E. M., Konen, E., Kiryati, N., & Mayer, A. (2017). Patient-specific image denoising for ultra-low-dose CT-guided lung biopsies. *International Journal of Computer Assisted Radiology and Surgery*, *12*(12), 2145–2155. doi:10.1007/s11548-017-1621-6 PMID:28601962

Hacking, C., & Cuete, D. (n.d.). *CT artifacts.* https://radiopaedia.org/articles/ct-artifacts

Kramer, O. (2017). *Genetic Algorithm Essentials* (Vol. 679). Springer. doi:10.1007/978-3-319-52156-5

Kumar, M., & Diwakar, M. (2016). CT image denoising using locally adaptive shrinkage rule in tetrolet domain. *Journal of King Saud University - Computer and Information Sciences, 30*(1), 41–50.

Manson, E. N., Ampoh, V. A., Fiagbedzi, E., Amuasi, J. H., Flether, J. J., & Schandorf, C. (2019). Image noise in radiography and tomography: Causes, effects and reduction techniques. *Current Trends in Clinical & Medical Imaging*, *2*(5), 555620. doi:10.19080/CTCMI.2019.02.555620

Mao, Q., & Zhao, S. G. (2020). Modified rolling-ball method for pulmonary parenchyma segmentation. *Journal of Medical Imaging and Health Informatics*, *10*(2), 364–369. doi:10.1166/jmihi.2020.2882

McCunney, R. J., & Li, J. (2014). Radiation risks in lung cancer screening programs: A comparison with nuclear industry workers and atomic bomb survivors. *Chest*, *145*(3), 618–624. doi:10.1378/chest.13-1420 PMID:24590022

Misiti, M., Misiti, Y., Oppenheim, G., & Poggi, J.-M. (2007). *Wavelet and Their Applications*. Wiley. doi:10.1002/9780470612491

Periyasamy, N., & Ramasamy, A. (2018). A novel edge preserving improved adaptive wavelet filter (EPIAWF) for speckle removal in ultrasound images. *Current Medical Imaging Reviews*, *14*(4), 521–532. doi:10.2174/15 734056136661701181021

Rathee, G., Sharma, A., Saini, H., Kumar, R., & Iqbal, R. (2020). A hybrid framework for multimedia data processing in IoT-healthcare using blockchain technology. *Multimedia Tools and Applications*, *79*(15-16), 9711–9733. doi:10.1007/s11042-019-07835-3

Schabath, M. B., Massion, P. P., Thompson, Z. J., Eschrich, S. A., Balagurunathan, Y., Goldof, D., Aberle, D. R., & Gillies, R. J. (2016). Differences in patient outcomes of prevalence, interval, and screen-detected lung cancers in the CT arm of the national lung screening trial. *PLoS One*, *11*(8), e0159880. doi:10.1371/journal. pone.0159880 PMID:27509046

Seddik, H. (2014). A new family of Gaussian filters with adaptive lobe location and smoothing strength for efficient image restoration. *EURASIP Journal on Advances in Signal Processing*, *2014*(1), 25. doi:10.1186/1687-6180-2014-25

Sharma, A., Ansari, M. D., & Kumar, R. (2017). A comparative study of edge detectors in digital image processing. In *2017 4th International Conference on Signal Processing, Computing and Control (ISPCC)* (pp. 246-250), doi:10.1109/ISPCC.2017.8269683

Shrestha, S. (2014). Image denoising using new adaptive based median filter. *Signal and Image Processing: an International Journal*, *5*(4), 1–13. doi:10.5121/sipij.2014.5401

Tiruwa, S., & Yadav, R. B. (2018). Comparing various filtering techniques for reducing noise in MRI. In *2018 International Conference on Sustainable Energy, Electronics and Computing System*. SEEMS 2018. doi:10.1109/ SEEMS.2018.8687345

Wang, Y., Shao, Y., Zhang, Q., Liu, Y., Chen, Y., Chen, W., & Gui, Z. (2017). Noise removal of low-dose CT images using modified smooth patch ordering. *IEEE Access: Practical Innovations, Open Solutions*, *5*, 26092–26103. doi:10.1109/ACCESS.2017.2777440

Zhang, H., Zeng, D., Zhang, H., Wang, J., Liang, Z., & Ma, J. (2017). Applications of nonlocal means algorithm in low-dose X-ray CT image processing and reconstruction: A review. *Medical Physics*, *44*(3), 1168–1185. doi:10.1002/mp.12097 PMID:28303644

Shabana Ziyad received BSc degree from P.S.G College of Technology, Coimbatore, India and later earned MCA degree from the same college in 2001.She was working in P.S.G.R Krishnammal college for Women, Coimbatore, India up to 2003. She continued working as a lecturer in Patrician College of Arts and Sciences, Adayar, Chennai, India up to 2006. She is working as a lecturer in Department of computer science at College of Engineering and Sciences in Prince Sattam bin Abdul Aziz University, Al-Kharj, KSA since 2012 till date. Her research interest are medical imaging and algorithms. She is now pursuing PhD in Computer Science at Avinashilingam Institute for Home Science and Higher Education for Women, India.

V. Radha, Professor Computer Science, Avinashilingam Institute for Home Science and Higher Education for Women, Coimbatore, Tamil Nadu, India. She has more than 29 years of teaching experience and 16 years of Research Experience. Her Area of Specialization includes Image Processing, Optimization Techniques, Speech Signal Processing, Data Mining & Data Warehousing and RDBMS. She has authored more than 110 papers published in refereed International journals and Conferences. She has obtained funding projects from UGC-MRP in the field of speech signal processing. She is a Reviewer of American Journal Operational Research and American Journal of Signal Processing. She is an Editor in Chief of International Journal of Computational Science and Information Technology (IJCSITY). She is the member of many international bodies such as IEEE, IAENG, AIRCC, IACSIT etc. Visited countries such as the USA, UK, and Singapore.

V. Thavavel received her Bachelor of Science degree from Madurai Kamaraj University, India in 1995. She later earned Master of Computer Applications degree from Madurai Kamaraj University, India in 1999. She pursued her studies in Master of Philosophy at Madurai Kamaraj University, India and got the degree in 2005.She received the Doctor of Philosophy degree from Madurai Kamaraj University, India, 2008.She was working as lecturer in Arul Anandar College, India from 1999 to 2000, later joined as Lecturer in Fatima College, India up to 2005. She worked as Associate Professor & Head, Department of Computer Applications. Karunya University from 2008-2013.She continued her career as Assistant Professor, Department of Computer Sciences, Prince Sultan University, Saudi Arabia from 2013 – 2016.She is now working for PRINCE Sattam Bin AbdulAziz University, Al-Kharj, Saudi Arabia.